NACA

RESEARCH MEMORANDUM

AN INVESTIGATION OF A METHOD FOR OBTAINING HYDRODYNAMIC DATA AT VERY HIGH SPEEDS WITH A FREE WATER JET

By Bernard Weinflash and John R. McGehee

Langley Aeronautical Laboratory
Langley Field, Va.

NATIONAL ADVISORY COMMITTEE
FOR AERONAUTICS

WASHINGTON

June 14, 1954

[redacted]

NATIONAL ADVISORY COMMITTEE FOR AERONAUTICS

RESEARCH MEMORANDUM

AN INVESTIGATION OF A METHOD FOR OBTAINING HYDRODYNAMIC DATA AT VERY HIGH SPEEDS WITH A FREE WATER JET

By Bernard Weinflash and John R. McGehee

SUMMARY

Information is presented on the feasibility of using a rectangular free water jet to obtain hydrodynamic data at very high speeds. The 3-inch by 3/4-inch jet investigated was actuated by compressed air which forced the water through a nozzle at speeds from about 80 to 200 ft/sec. Total-head pressure distributions in the jet up to 8 inches downstream of the nozzle exit are presented and experimental hydrodynamic lift data are given for two models planing on the 3-inch-wide surface of the jet. These planing data are compared with similar data obtained in the Langley towing tanks.

The data obtained in this investigation indicate that it is feasible to use a free water jet as a hydrodynamic test facility for obtaining planing data at very high speeds. The main problem appears to be the establishment of an adequate method of correcting the jet data for the limited boundaries of a reasonable-size jet. Consideration has been given to a simple empirical method of correcting planing data for the jet boundaries. This method gave reasonable results for the limited data available.

INTRODUCTION

The rapid increase in the landing speeds of current airplanes has caused a corresponding increase in the water speeds at which seaplanes operate. As a result, the gap between the speeds available in existing hydrodynamic testing facilities and full-scale speeds has widened to an extent sufficient to make it advisable to ascertain whether these differences in speed are causing any significant differences in force coefficients. In an attempt to close this gap, an investigation has been made of the feasibility of obtaining hydrodynamic data at full-scale speeds by utilizing a rectangular free water jet actuated by compressed air.

[redacted]

A small model of such a test facility with a nozzle 3 inches wide by 3/4 inch deep was constructed and the jet characteristics investigated for speeds from 80 to 200 ft/sec. In order to obtain some indication of the potentialities of the jet as a hydrodynamic test facility, hydrodynamic lift forces were measured on two models, one having a flat bottom and the other a complex bottom, planing on the 3-inch-wide surface of the jet.

SYMBOLS

A	average acceleration through nozzle, ft/sec^2
a	acceleration at a given cross section in nozzle, ft/sec^2
b	beam of models, in.
C_L	hydrodynamic lift coefficient
C_{L_1}	hydrodynamic lift coefficient obtained from jet data, $\frac{288L}{\rho l b V^2}$
C_{L_2}	hydrodynamic lift coefficient obtained from tank data
d	draft at trailing edge of model (measured from upper edge of nozzle exit), in.
h	height of trailing edge of model above lower edge of jet, $2Z - d$, in.
L	lift, lb
l	wetted length, $d/\sin \tau$, in.
P	static pressure in tank at level of nozzle, lb/sq in. (gage)
p	static pressure at given cross section in nozzle, lb/sq in. (gage)
q	dynamic pressure in jet, lb/sq in. (gage)
S	area of nozzle exit, sq in.
s	area of given cross section in nozzle, sq in.

[redacted]

V speed equivalent to static pressure in tank at level of nozzle, $\sqrt{\frac{144P}{\rho/2}}$, ft/sec

V_q speed in jet equivalent to measured dynamic pressure, $\sqrt{\frac{144q}{\rho/2}}$, ft/sec

v speed at a given cross section of nozzle, ft/sec

X length of contracting section of nozzle, 8.5 in.

x distance downstream of nozzle entrance measured along nozzle axis, in.

x' distance downstream of nozzle exit measured along nozzle axis, in.

y transverse distance from vertical plane of symmetry of nozzle at a given cross section, in.

Z half vertical dimension of nozzle exit, 0.375 in.

z vertical distance from horizontal plane of symmetry of nozzle at a given cross section, in.

τ trim (angle between model reference line and horizontal), deg

ρ mass density of water, 1.94 slugs/cu ft

APPARATUS AND PROCEDURE

Facility

A schematic drawing of the jet apparatus is shown in figure 1. High-pressure air is used to force water from the tank through the nozzle to form the free-jet test section. The water tank consists of a seamless steel tube capped at both ends and holds about 25 cubic feet of usable water volume. A diffuser at the tank end of the air line prevents the air from impinging directly on the water surface and mixing turbulently with the water. A pressure transmitter picks up the static pressure at the nozzle and records it on the oscillograph. The over-all response of the pressure recording apparatus is approximately 40 cps.

[redacted]

Details of the nozzle are given in figure 2. All sides of the contraction have the same elliptical shape and are within the limit for noncavitating flow set up for elliptical profile contractions in reference 1. The elliptical profiles fair smoothly into a flat surface built up on the inner surface of the cylindrical tank. The calculated variation of area, speed, acceleration, and static pressure along the length of the contracting section are plotted in nondimensional form in figure 3. The sharp changes in the slope of the speed and acceleration curves near the nozzle entrance do not indicate what occurs in reality. Actually, the water begins moving horizontally somewhere upstream of the nozzle entrance.

A picture of the water jet flowing at 130 ft/sec is shown in figure 4. The pressure gage shown measures the static pressure at the nozzle entrance but has an equivalent speed scale superimposed on the pressure scale.

Total-Head Pressure Survey

The apparatus used in making a total-head pressure survey of the water jet is shown in figure 5. A total-head tube having an outside diameter of 0.03 inch and an inside diameter of 0.02 inch was attached perpendicular to the leading edge of a streamline strut so that the tube projected 0.25 inch in an upstream direction. The strut had a chord of 0.5 inch and a maximum thickness of 0.06 inch. The strut was mounted vertically between two transverse lead screws geared to the shaft of a constant-speed motor which drove the strut and total-head tube in a transverse direction at a rate of about 0.8 in./sec. The transverse location of the total-head tube relative to the vertical inner edge of the nozzle exit was recorded, by means of a cam-operated microswitch, simultaneously with the total-head pressure at the tube and with the static pressure in the tank at the level of the nozzle. Pressure-survey tests were made with a constant tank pressure so as to obtain constant jet speeds.

Dynamic-pressure surveys of jet cross sections were made at stations 0.5, 4, and 8 inches downstream of the nozzle exit x' for jet speeds of approximately 80, 130, and 200 ft/sec. At each longitudinal station the transverse pressure distribution was recorded at a number of vertical positions z. Because the jet was considered symmetrical, only one-quarter of its cross-sectional area was investigated as shown in figure 5.

Since the effect of gravity on the jet may be neglected (for $x' = 8$ inches, a particle of water emitted from the jet at 200 ft/sec will drop 0.002 inch; and at 80 ft/sec 0.013 inch), extensions of the planes of symmetry of the nozzle were taken as the planes of symmetry

for the jet also. Three records taken at a distance of 4 inches downstream of the nozzle exit for a speed of about 200 ft/sec are shown in figure 6 for $z = 0$, 0.325, and 0.375. These figures show the simultaneous records made by the position recorder and the pressure transmitters.

Model Tests

The technique used to make tests for obtaining planing data was a little different from that used to make pressure surveys. An initial charge of high-pressure air was sealed off in the top of the water tank so that when the nozzle was opened the decreasing water level allowed this air to expand. The corresponding decrease in pressure resulted in a gradual decrease in jet speed. This gradual decrease in speed made it possible to cover a speed range from 200 to 80 ft/sec in a single test.

Hydrodynamic lift was measured for a flat-bottom model having a 1-inch beam and for a complex-bottom model having a variable beam averaging approximately 1 inch. The models are shown in figure 7 and photographs of the models planing on the 3-inch-wide surface of the jet are shown in figure 8. Tests were made at trims of 8° and 12° for wetted length-beam ratios of 1, 2, 3, and 4 except that, at 12°, a wetted length-beam ratio of 3.6 was used because higher values would cause the trailing edge of the model to project through the bottom surface of the jet. Lift forces were recorded on the oscillograph simultaneously with the static pressure in the tank.

Trim was measured as the angle between the model reference line and the horizontal. Draft was the vertical distance between the trailing edge of the planing surface and the nominal jet surface (taken as the upper edge of the nozzle exit). Wetted length was obtained by dividing the draft by the sine of the angle of trim. The wetted area used in obtaining lift coefficients was the product of this wetted length and the beam (1 inch). The speed V was obtained from the formula

$$V = \sqrt{\frac{144P}{\rho/2}}$$

where P was the static gage pressure in the tank.

RESULTS AND DISCUSSION

General

Figure 9 shows top and side photographs, taken simultaneously, of the flow at 200 ft/sec through a transparent plastic extension of the

nozzle (2.5 inches long). The sharp picture of the star pasted to the underside of the extension demonstrates the clarity of flow before it came in contact with the atmosphere. (The cloudy streak appearing in one corner was due to imperfect alinement of the extension with the nozzle exit.) As soon as the water emerged from the extension its surface immediately became streaked with white. This experiment indicates that the whitish appearance of the jet is due to entrainment of the surrounding air and not due to the release of air from the jet as the pressure dropped to that of the atmosphere in the straight portion of the nozzle and its extension.

Dynamic Pressure Distribution

In order to make the results readily comparable to the conventional boundary-layer plots for incompressible flows, the total-head survey data are presented as the speed ratio V_q/V. The value of V_q is the speed that would be obtained if all the jet were water only. In the region where air and water are mixed, however, the density is less than that of water and V_q is not strictly the speed in that region.

Three of the transverse speed distributions obtained parallel to the wide surface, 4 inches downstream of the nozzle exit ($x' = 4$) at a speed of 200 ft/sec, are shown in figure 10(a). These curves were obtained from the three records shown in figure 6. They show the pressures in the plane of symmetry ($z = 0$), in a plane 0.05 inch from the edge of the nozzle ($z = 0.325$), and in a plane at the edge of the nozzle (nominal surface, $z = 0.375$). Corresponding vertical distributions parallel to the narrow surface of the jet are shown in figure 10(b). Vertical distributions for $y = 0.7$ and 1.0 also are shown in this figure. These data were obtained from all the transverse records taken at $x' = 4$ inches and $V = 200$ ft/sec.

In general, the jet appeared to consist of a sizable core of total-pressure conversion where V_q equaled V and a surface zone where V_q decreased from V to zero. Probably a large part, if not substantially all, of the surface zone was a mixture of water and entrained air. The gradation in dynamic pressure on the surface thus may be due to changes in density as well as speed. If necessary, this mixing zone on the surface probably could be reduced substantially either by operating the jet in a vacuum or by blowing air over the surface of the jet in the direction of flow.

In figure 10 the speed-ratio distributions show a sharp change through the surface and then the ratio V_q/V remains steady at a value of 1 for both the wide and narrow surfaces. The speed-ratio distributions 0.05 inch from the nominal surfaces show the speed variation near the

inner boundary of the mixing zone in the center section of the jet. In the flat portion of these curves, the ratio V_q/V was about 1 for the wide surface and about 0.93 for the narrow surface. The speed-ratio distributions at the nominal surfaces show the speed variation inside the mixing zone. On the wide nominal surface, most of the curve was still roughly flat with an average V_q/V of about 0.85. On the narrow nominal surface there was no flat portion to the curve and the highest value was about 0.6. Fluctuations in values of speed ratio similar to those shown in the curve for $z = 0.375$ inch in figure 10(a) possibly would have appeared in the corresponding curve for $y = 1.50$ inches in figure 10(b), had pressure traverses been made at more vertical stations between $z = 0$ and $z = 0.3$ inch.

Cross sections through the jet taken 0.5, 4, and 8 inches downstream of the nozzle exit at speeds of approximately 80, 130, and 200 ft/sec are shown in figure 11. Longitudinal sections through the horizontal and vertical planes of symmetry are shown in figure 12. Faired contours of constant speed ratios are plotted for V_q/V of 0, 0.2, 0.4, 0.6, 0.8, and 1.0. The outline of the nozzle exit is included to show the location of the nominal surfaces. Within the scope of this investigation, the variations in jet characteristics with speed were minor and did not appear to establish a consistent trend.

The thickness of the mixing zone just downstream of the nozzle exit ($x' = 0.5$ inch) was the same for the wide and the narrow surfaces, about 0.1 inch. With increase in distance downstream of the nozzle exit to $x' = 4$ inches, the thickness of the mixing zone on the wide surface did not increase much; but on the narrow surface it approximately doubled. With further increase in distance downstream of the nozzle exit to $x' = 8$ inches, the thickness of the mixing zone on both the wide and narrow surfaces increased to approximately double the thickness at $x' = 4$ inches. The thicker mixing zone on the narrow surface probably was due, for the most part, to the thickening at the corners.

Just downstream of the nozzle exit ($x' = 0.5$ inch) the width of the center section of the jet surface, for which the mixing-zone characteristics remained fairly unchanged, was about 90 percent of the 3-inch-wide surface and about 80 percent of the 3/4-inch-wide surface. With increase in x' to 8 inches, the width of the center section decreased to about 60 percent for the wide surface and to about 25 percent for the narrow surface.

Planing Tests

Planing lift coefficients for the flat-bottom model, obtained in the jet at 80 ft/sec, are given in table I, together with comparable data obtained in Langley tank no. 1. Data are presented for trims of 8° and 12° (fig. 13) and wetted length-beam ratios of 1, 2, 3, 3.6, and 4. The towing-tank data were taken from reference 2 and are for a model 4 inches wide. In figure 13, the ratios of the lift coefficient obtained in the tank to that obtained in the jet C_{L_2}/C_{L_1} are plotted against the ratio of the height of the trailing edge of the model above the lower jet boundary to the wetted length h/l. The data fell close to a single curve for the trims and length-beam ratios investigated.

According to this curve, the lift coefficient obtained in the tank C_{L_2} was about 2.3 times that obtained in the jet C_{L_1} when the planing surface penetrated the jet to its lower boundary $h/l = 0$. As the trailing edge was moved up, away from the lower jet boundary (h/l increased), the ratio C_{L_2}/C_{L_1} decreased to about 1.2 at h/l of about 0.6. The lift coefficients obtained in the tank were always greater than those obtained in the jet. These results indicate that the variation of the ratio C_{L_2}/C_{L_1} with h/l may be due primarily to the boundaries of the limited jet stream. If so, the curve in figure 13 should be applicable as a jet correction factor for flat-bottom planing models and perhaps other types.

Planing lift coefficients for the complex-bottom model obtained in the jet at about 80 ft/sec are given in table II, together with comparable data obtained in Langley tank no. 2. Data are presented for a trim of 9° and wetted lengths of 1, 1.5, 2, 3, and 4. The towing-tank data were taken from unpublished data and are for a model averaging approximately 2.5 inches in width. The lift coefficients obtained in the jet at several values of h/l for the complex-bottom model were multiplied by the corresponding value of C_{L_2}/C_{L_1} obtained for the flat-bottom model (fig. 13).

In figure 14 these "corrected" values of C_L are compared with the lift coefficients obtained in the tank. The good agreement between the jet data corrected in this way and the tank data indicates that the simple correction procedure used may be broadly applicable. However, these data are not of sufficient scope to establish the limitations of this procedure.

CONCLUDING REMARKS

The data obtained in this investigation indicate that it is feasible to use a free water jet as a hydrodynamic test facility for obtaining planing data at very high speeds. The main problem appears to be the establishment of an adequate method of correcting the jet data for the limited boundaries of a reasonable-size jet. Consideration has been given to a simple empirical method of correcting planing data for the jet boundaries. This method gave reasonable results for the limited data available.

Langley Aeronautical Laboratory,
National Advisory Committee for Aeronautics,
Langley Field, Va., April 8, 1954.

REFERENCES

1. Rouse, Hunter, and Hassan, M. M.: Electrical Analogy Facilitates Design of Cavitation-Free Inlets and Contractions. State Univ. of Iowa, Inst. of Hydraulic Res., 1949.

2. Weinstein, Irving, and Kapryan, Walter J.: The High-Speed Planing Characteristics of a Rectangular Flat Plate Over a Wide Range of Trim and Wetted Length. NACA TN 2981, 1953.

TABLE I.- EXPERIMENTAL PLANING DATA OBTAINED FOR A FLAT-BOTTOM MODEL AT A SPEED OF 80 FT/SEC

τ, deg	l/b	$C_{L_{tank}}$	$C_{L_{jet}}$
8	1	[a]0.132	0.110
8	2	[a].100	.061
8	3	[a].080	.045
8	4	[a].071	.034
12	1	.214	.176
12	2	.158	.103
12	3	.135	.068
12	3.6	.124	.055

[a]Crossfaired data.

TABLE II.- EXPERIMENTAL PLANING DATA OBTAINED FOR A COMPLEX-BOTTOM MODEL AT A SPEED OF 80 FT/SEC

τ, deg	l/b	$C_{L_{tank}}$	$C_{L_{jet}}$ (a)
9	1	0.107	0.095
9	1.5	.103	.077
9	2	.097	.065
9	3	-----	.052
9	4	-----	.043

[a]Crossfaired data.

[redacted]

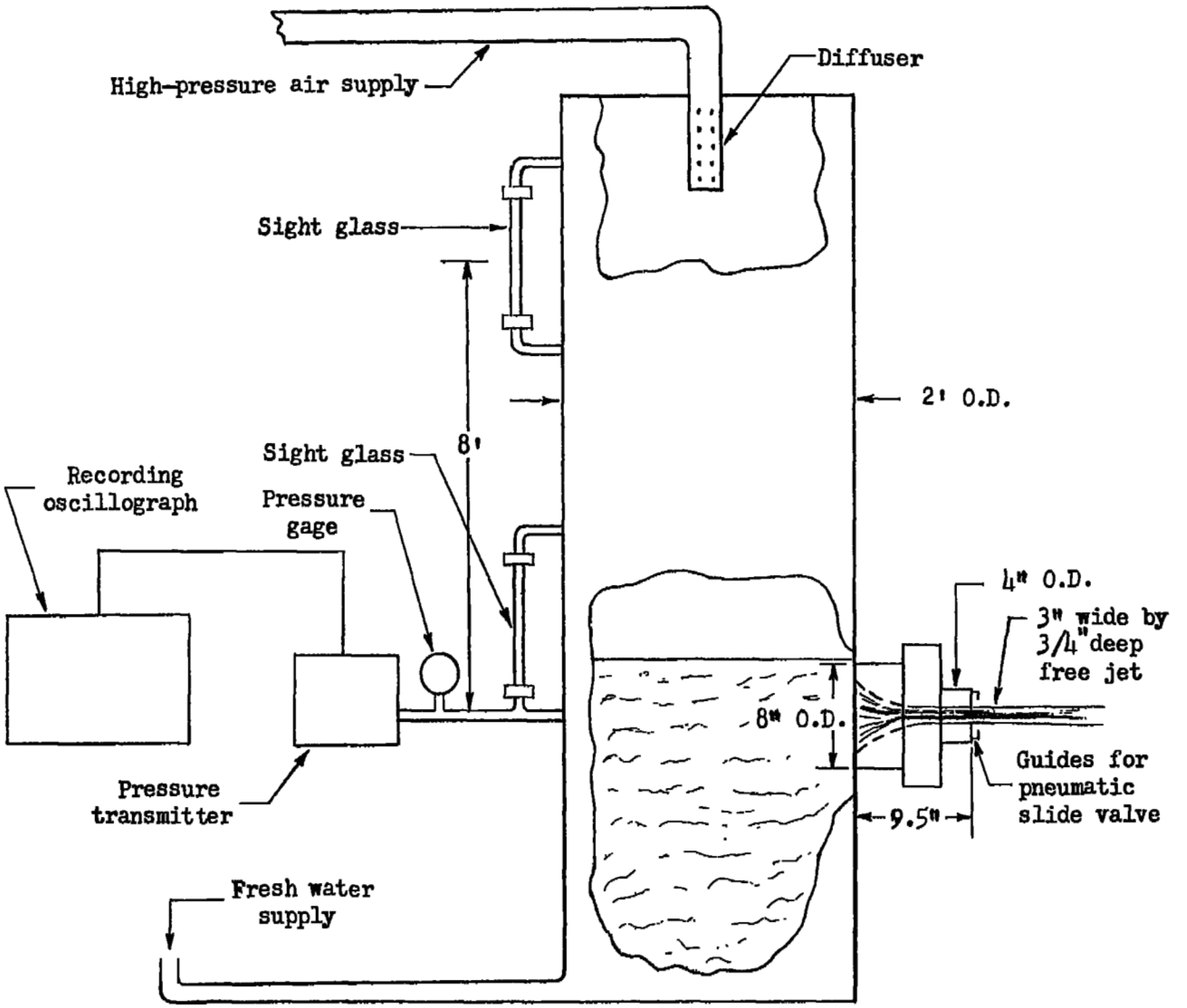

Figure 1.- Schematic drawing of equipment.

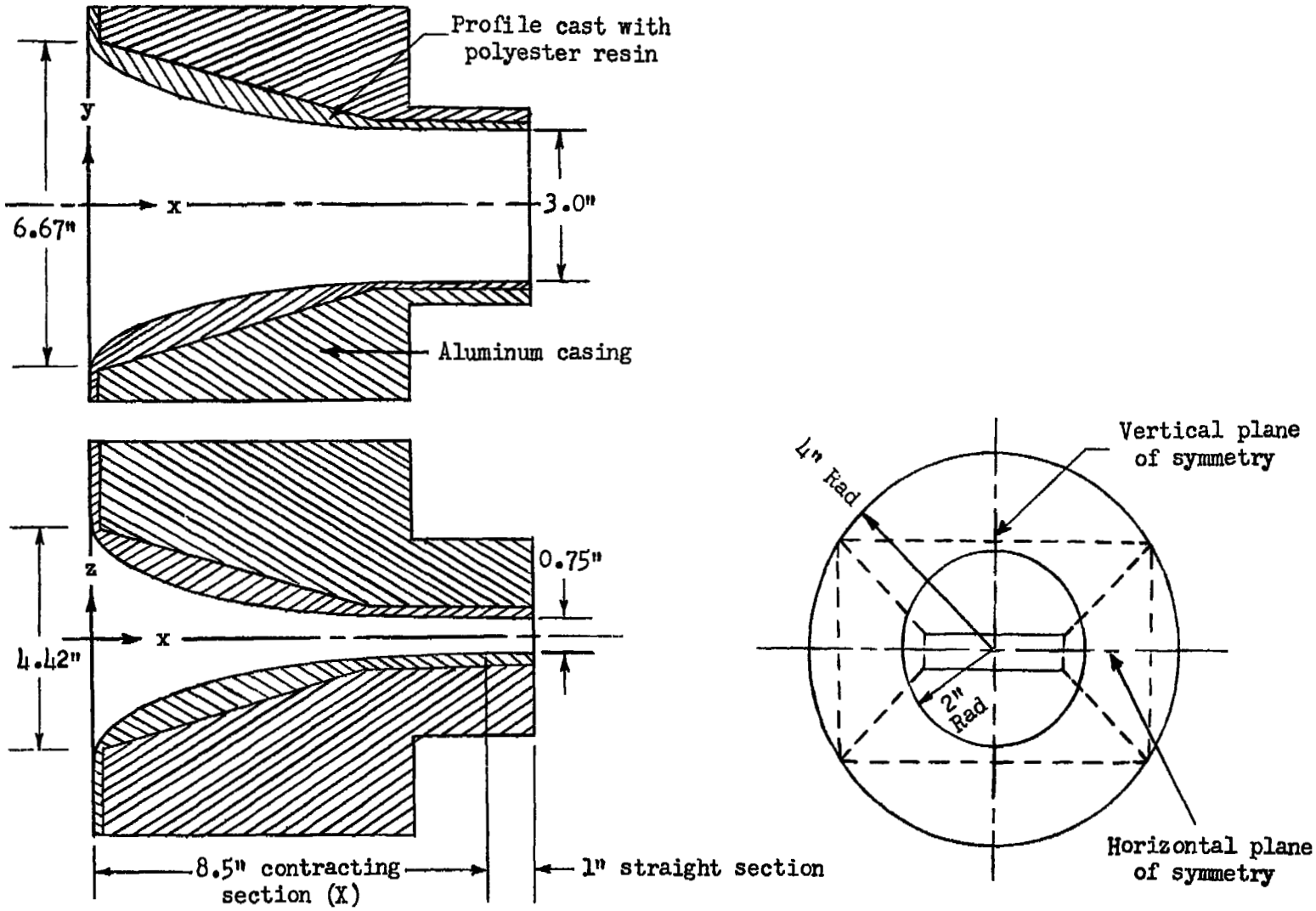

Figure 2.- Jet nozzle.

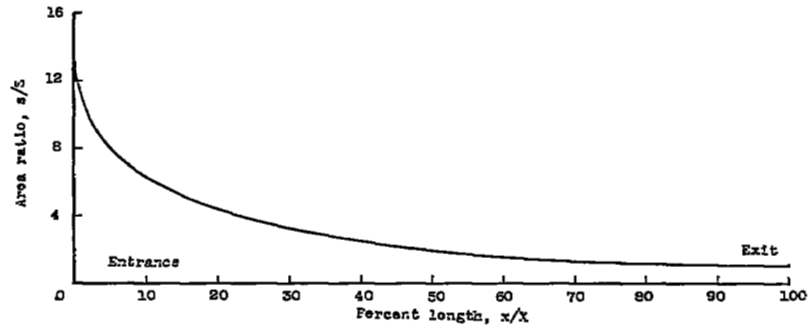

(a) Area ratios.

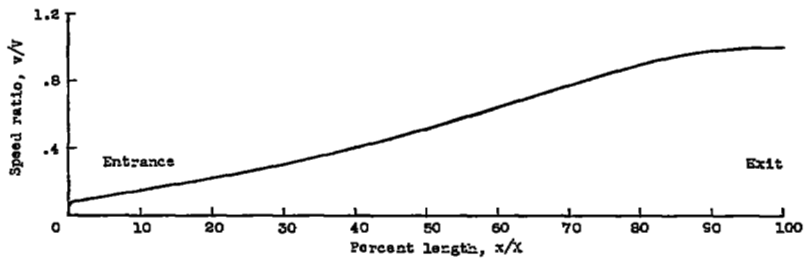

(b) Speed ratios.

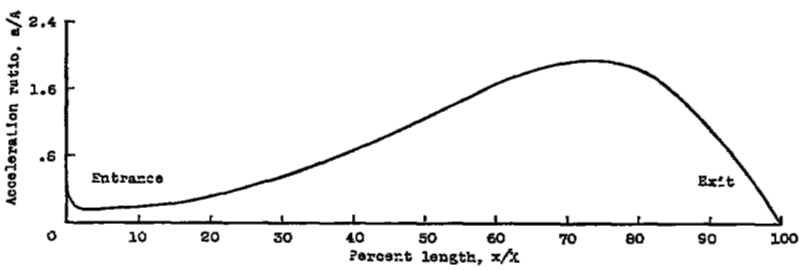

(c) Acceleration ratios.

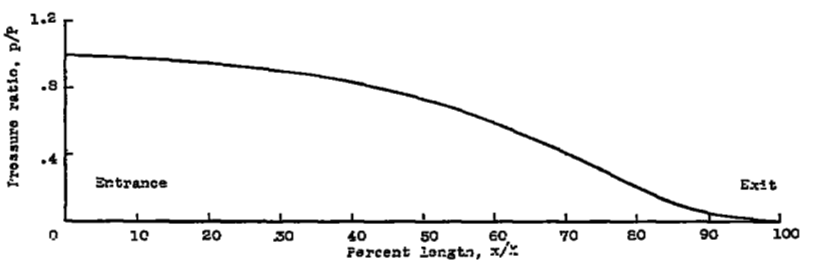

(d) Pressure ratios.

Figure 3.- Calculated nozzle characteristics.

[redacted]

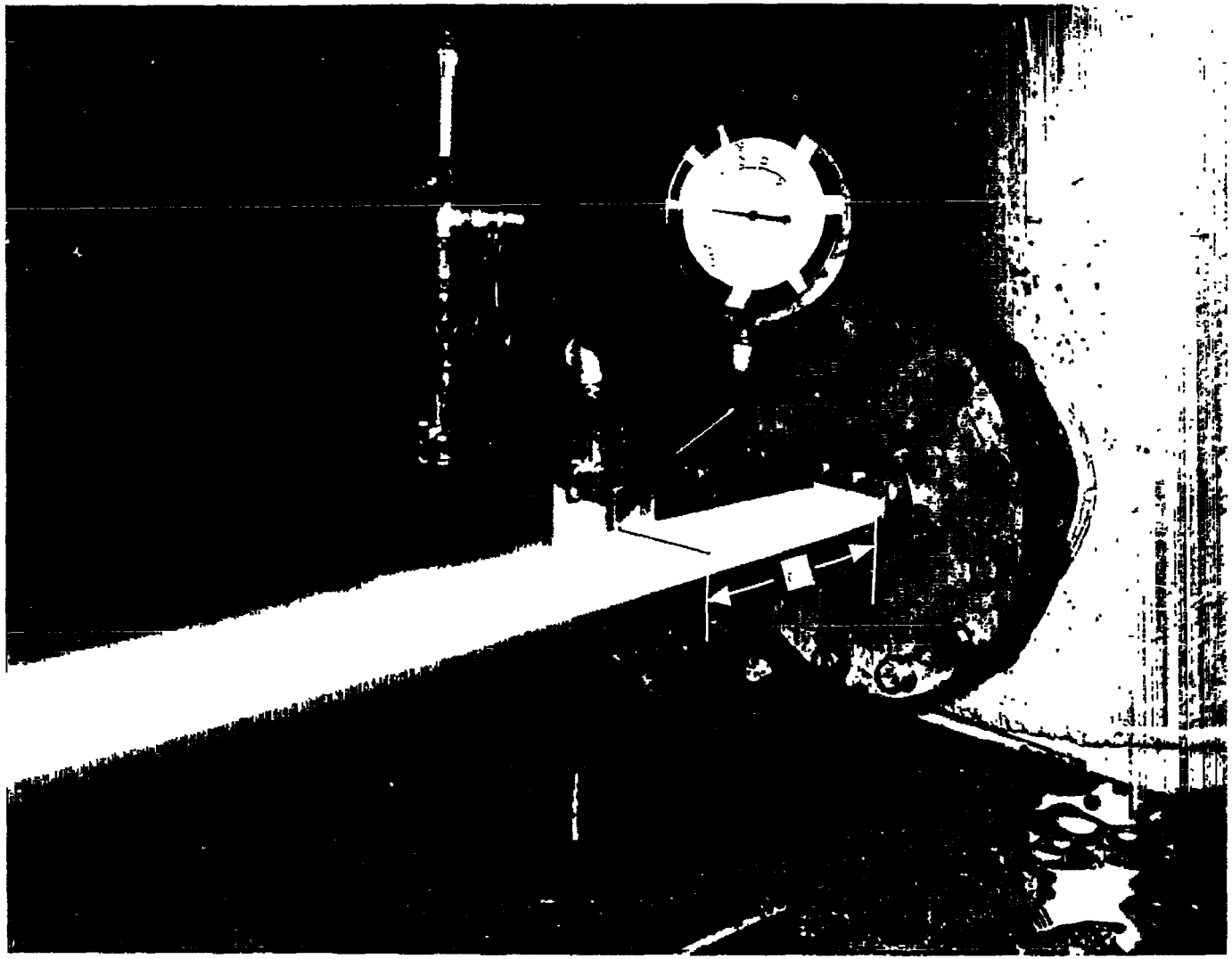

L-83649

Figure 4.- View of jet at a speed of 130 ft/sec.

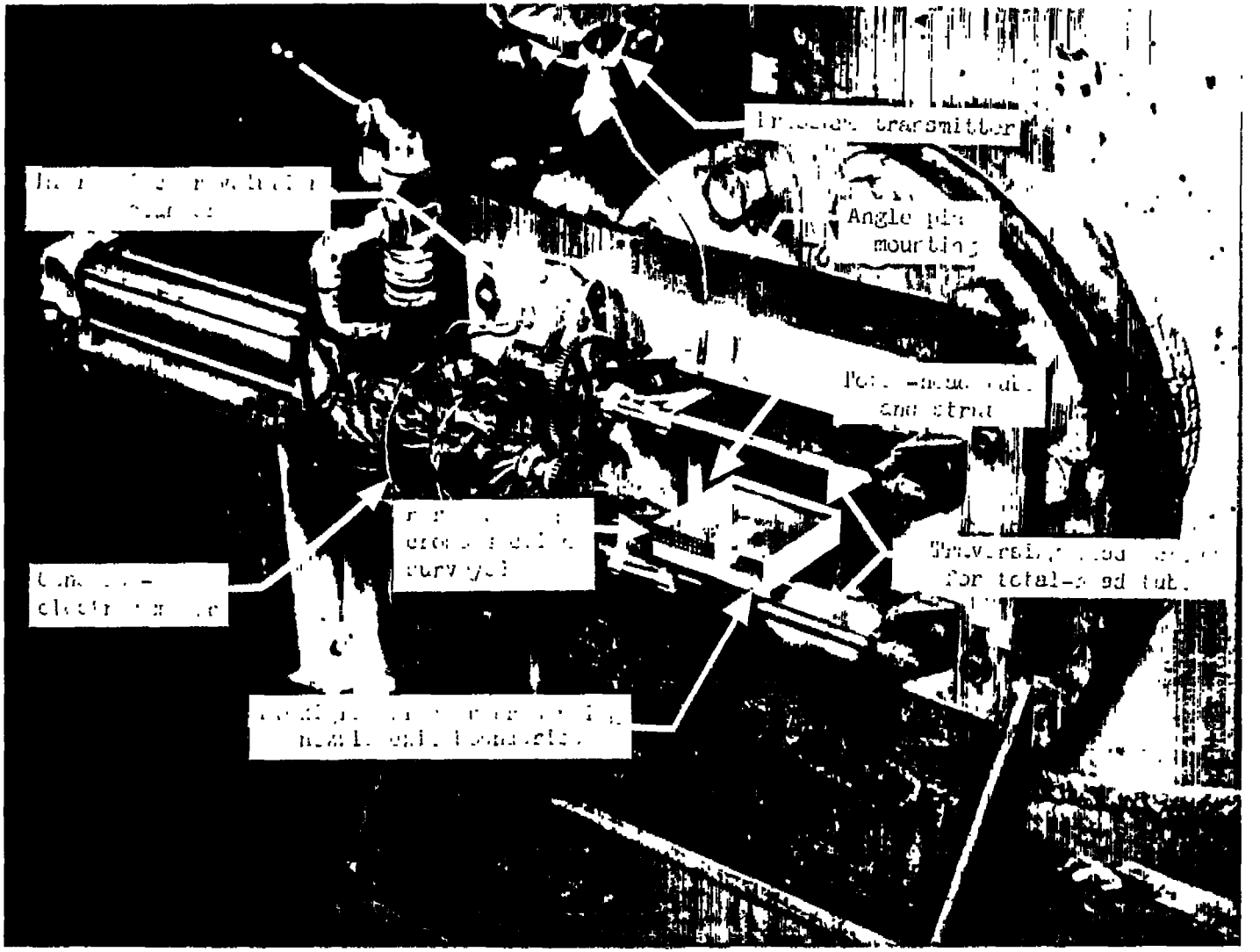

L-83650

Figure 5.- Apparatus for making total-head pressure survey.

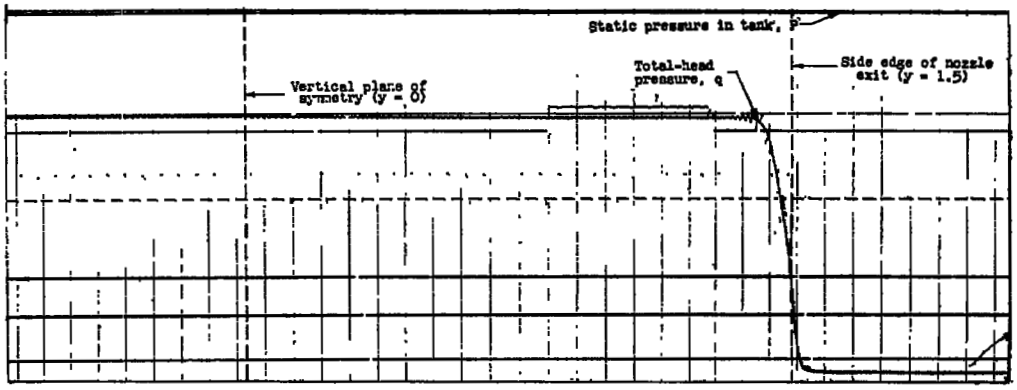

(a) z = 0.

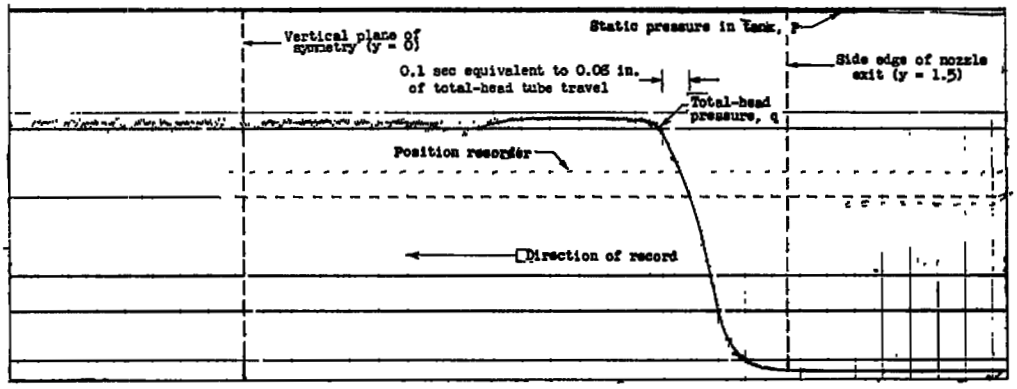

(b) z = 0.325 inch.

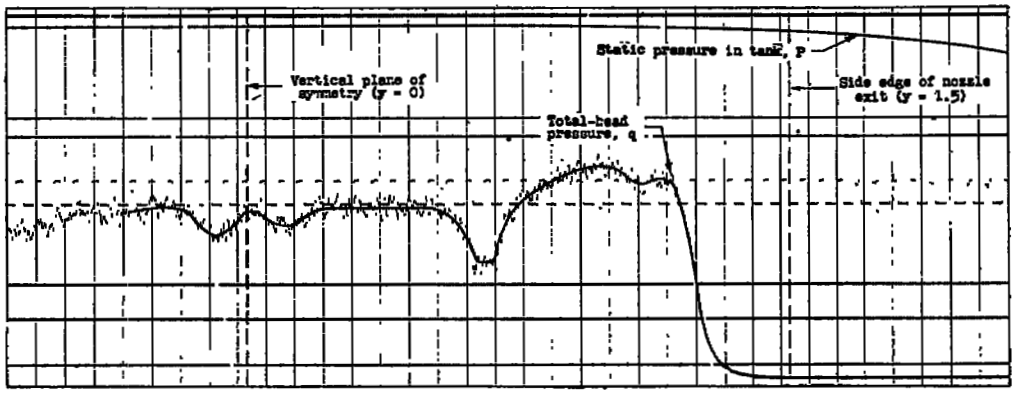

(c) z = 0.375 inch.

Figure 6.- Records of transverse total-head pressure distribution taken 4 inches downstream of nozzle exit at about 200 ft/sec.

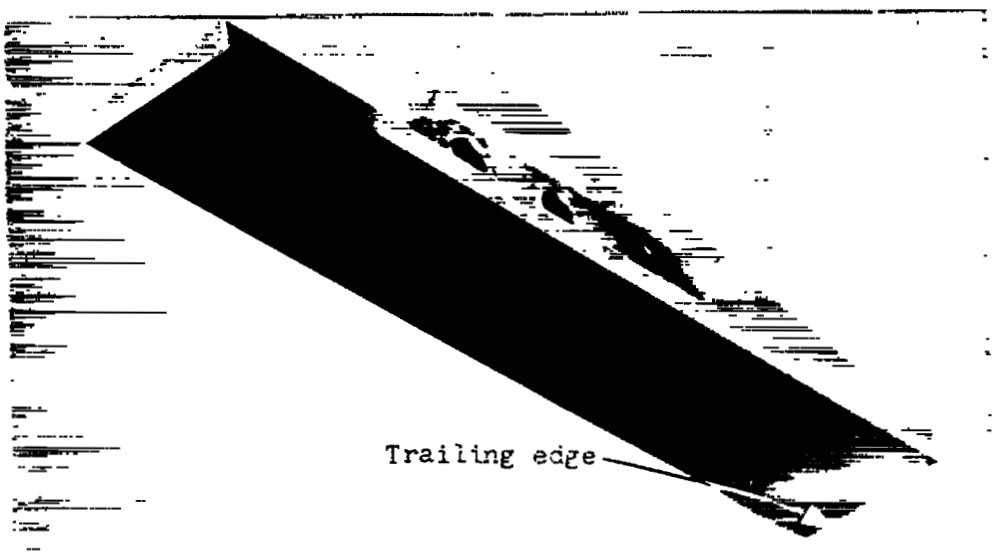

L-80865.1

(a) Flat-bottom model.

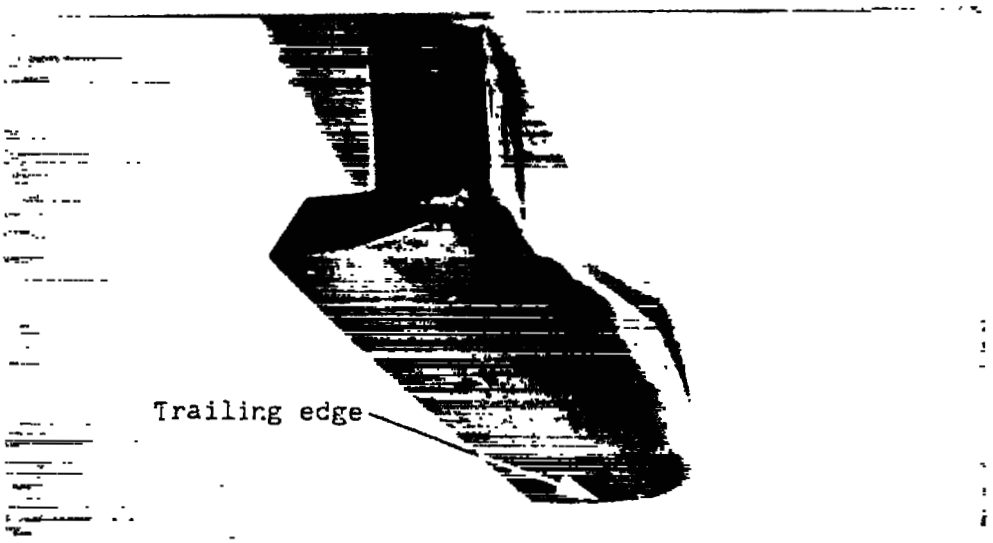

L-79654.1

(b) Complex-bottom model.

Figure 7.- Models tested.

200 fps

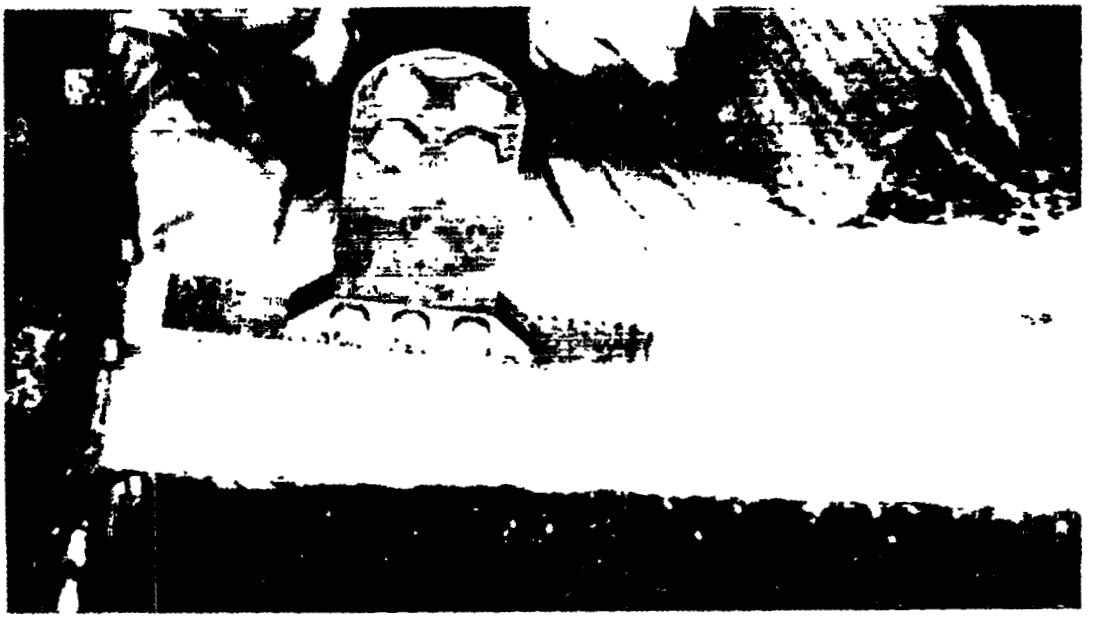

80 fps

L-83651

(a) Flat-bottom model.

Figure 8.- Photographs of models planing on jet. Trim, 8°; wetted-length-beam ratio, 2.

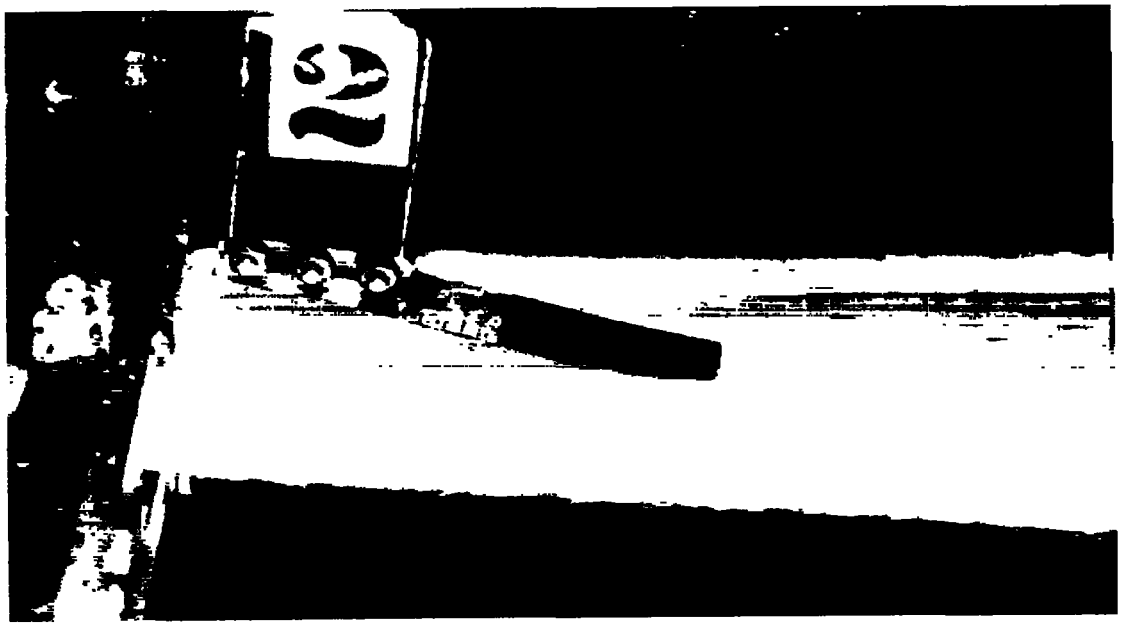

200 fps

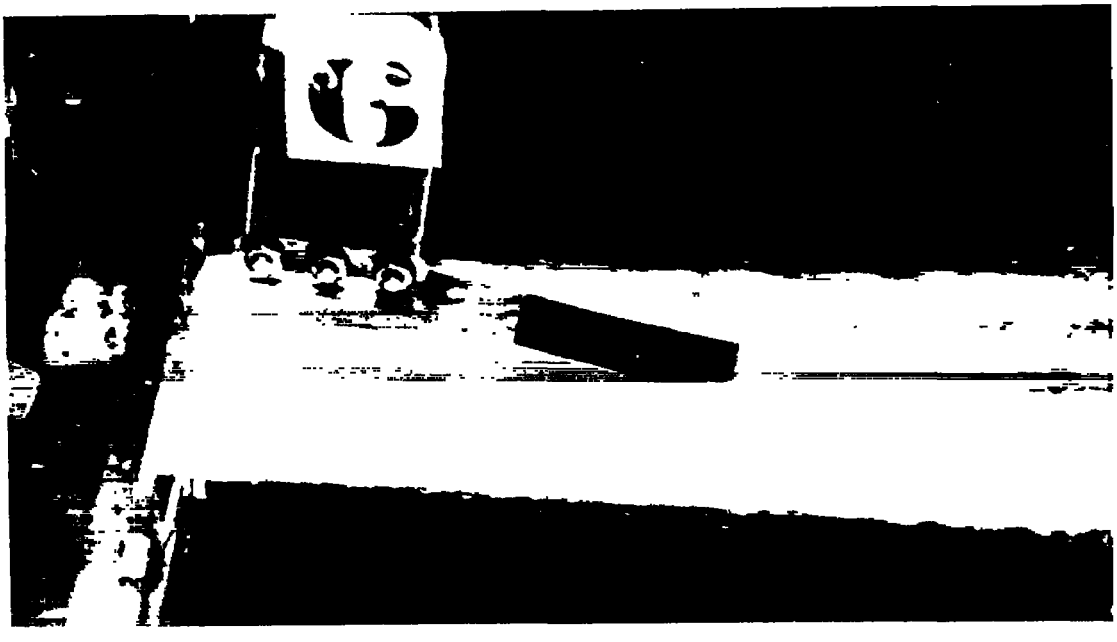

80 fps

L-83652

(b) Complex-bottom model.

Figure 8.- Concluded.

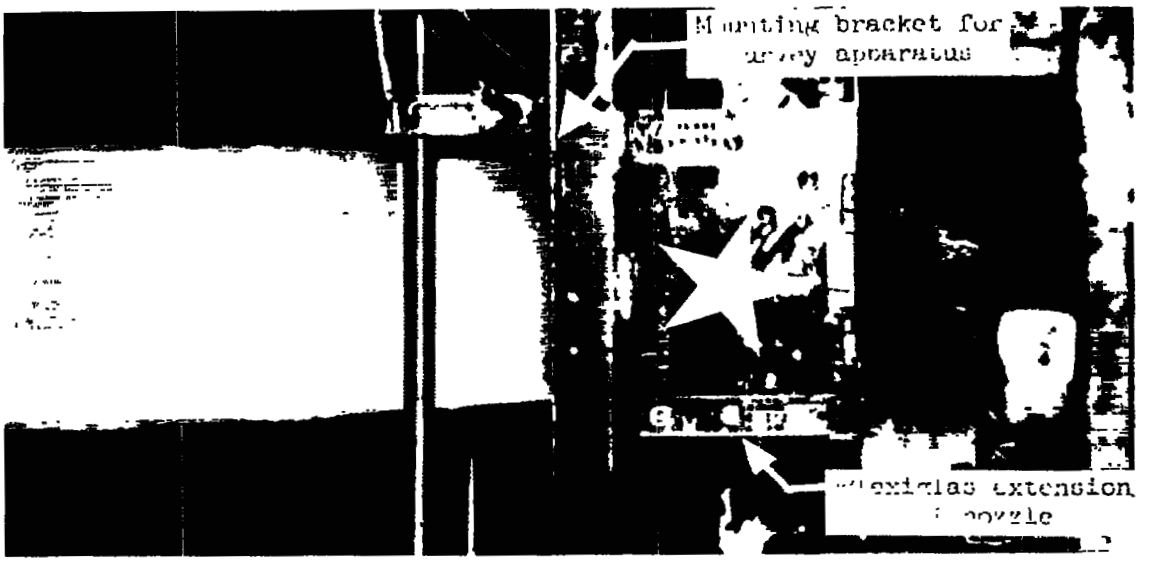

Top view

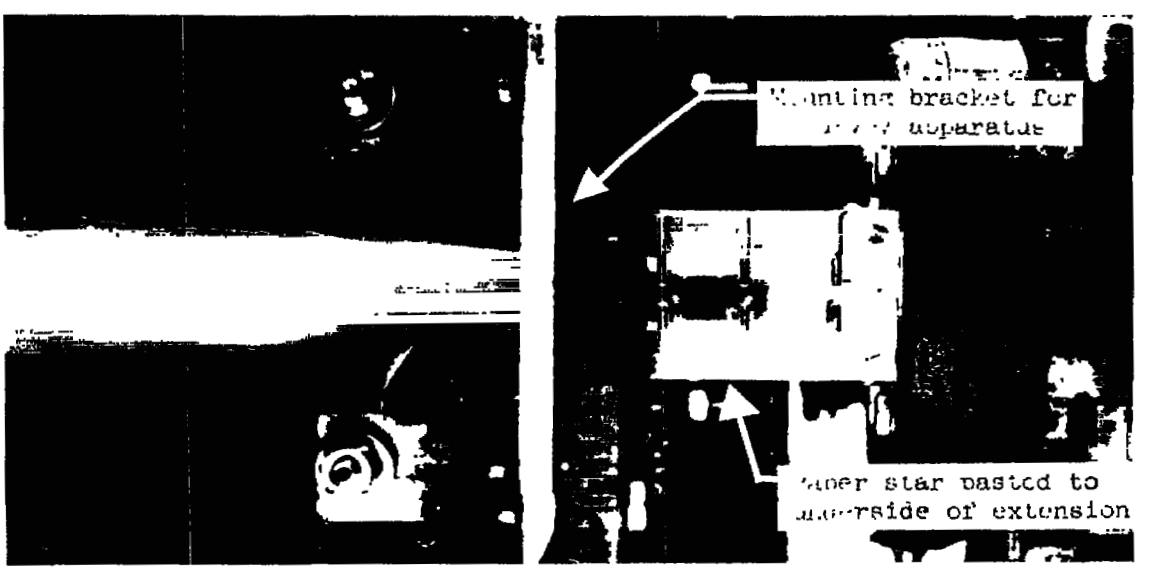

Side view

L-83653

Figure 9.- Entrainment of air (V = 200 ft/sec).

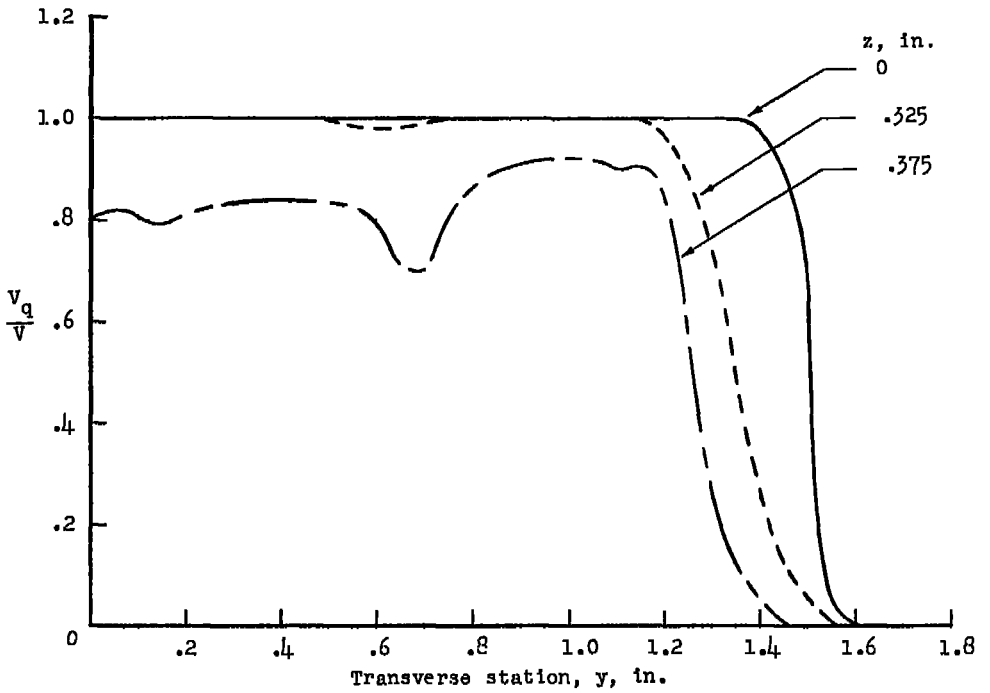

(a) Transverse stations along wide surface.

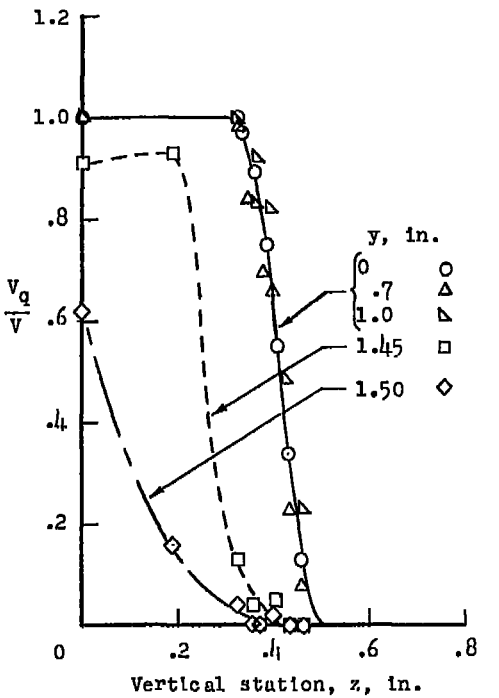

(b) Vertical stations along narrow surface.

Figure 10.- Speed-ratio variations in jet cross section. $x' = 4$ inches; V = approximately 200 ft/sec.

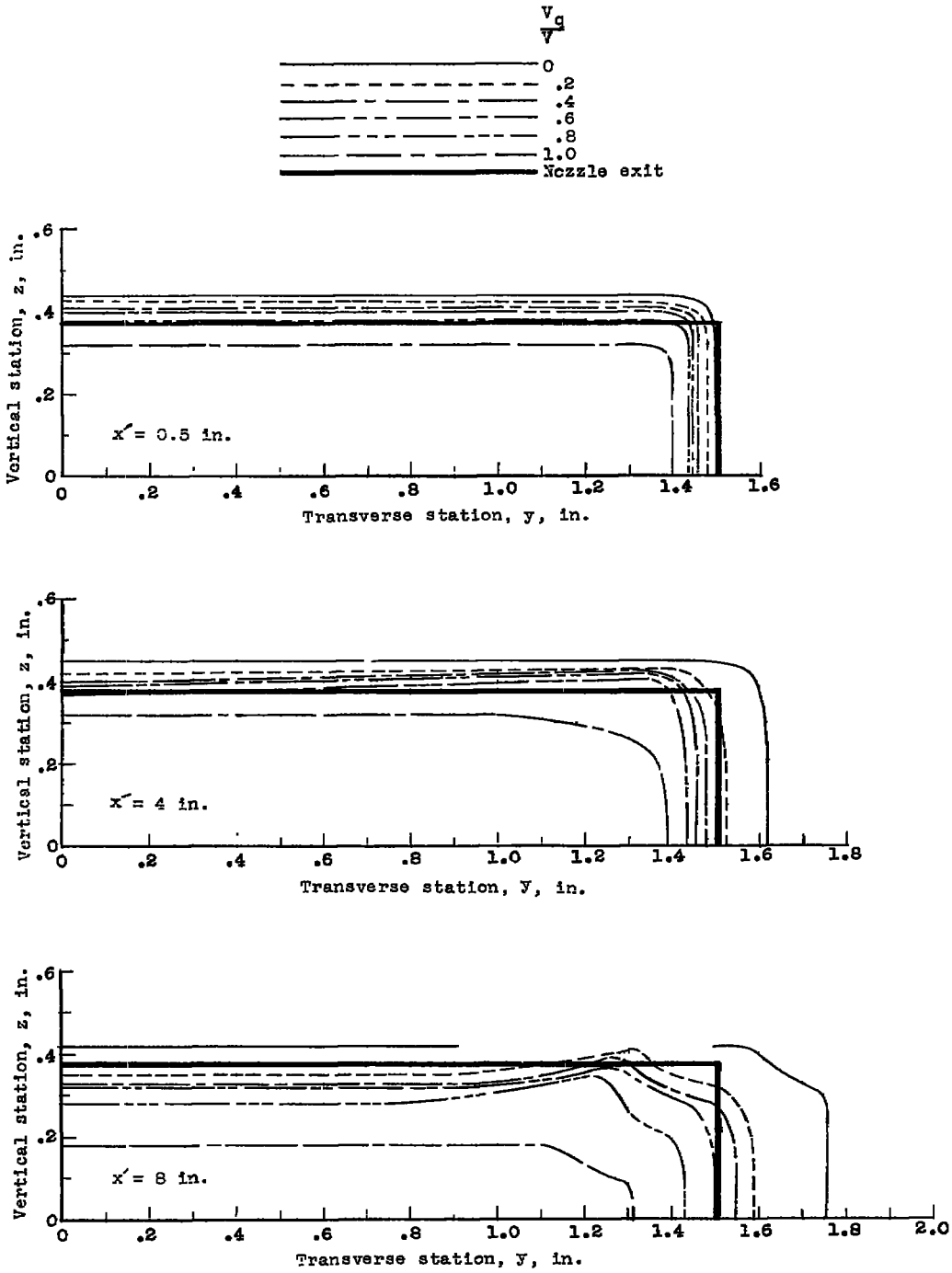

(a) Speed, 80 ft/sec.

Figure 11.- Cross section through jet showing contours of constant-speed ratio.

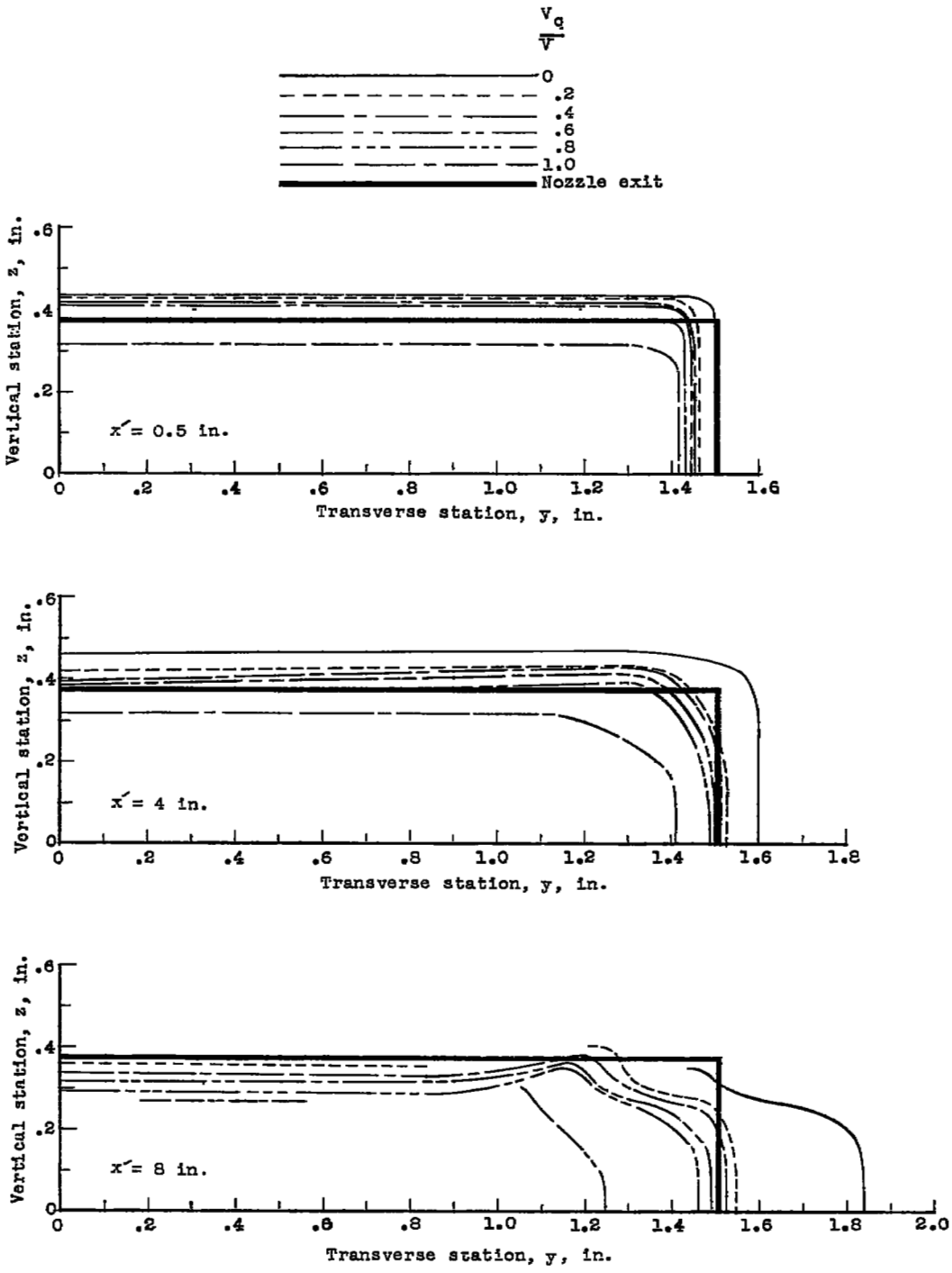

(b) Speed, 130 ft/sec.

Figure 11.- Continued.

[redacted]

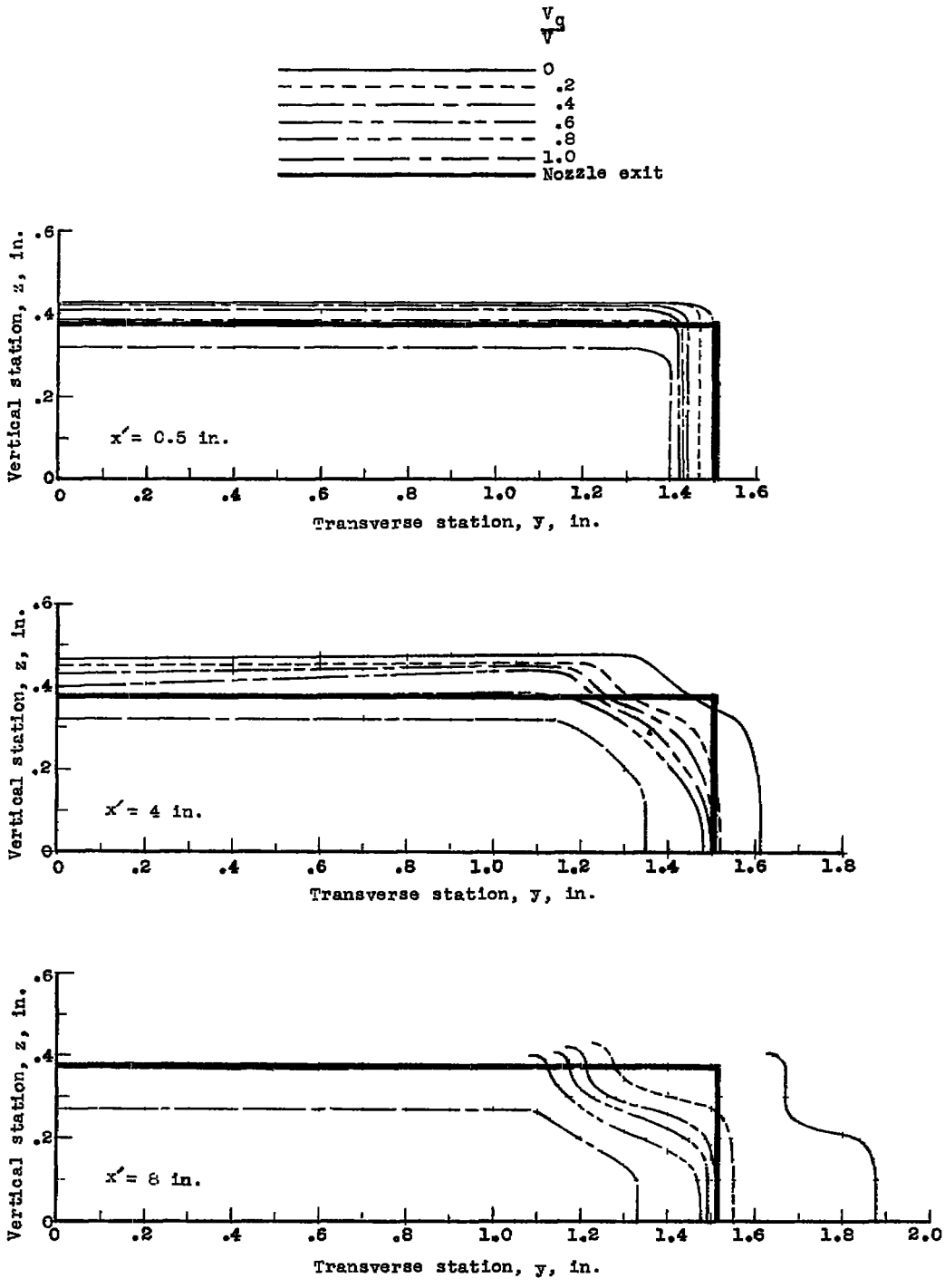

(c) Speed, 200 ft/sec.

Figure 11.- Concluded.

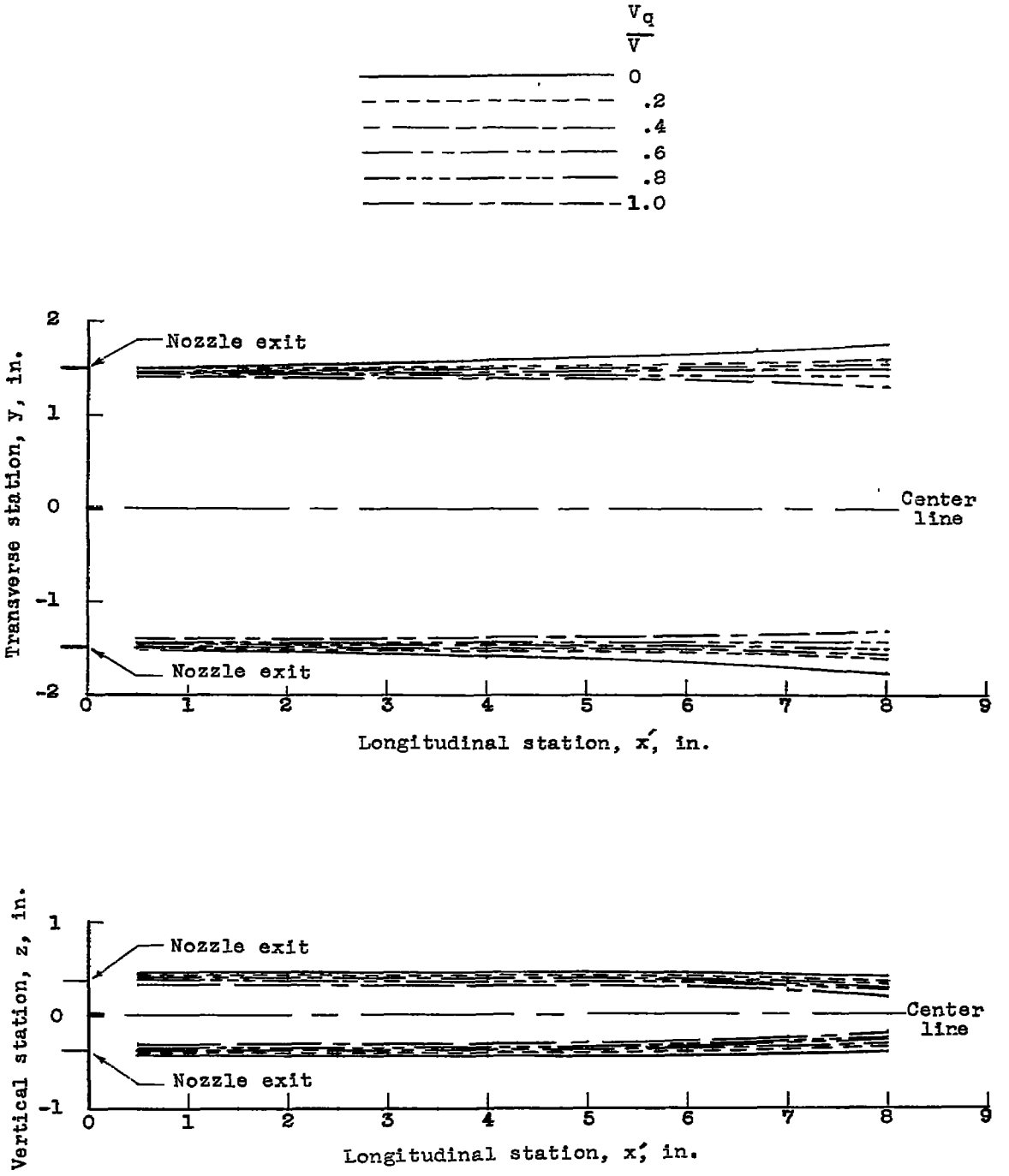

(a) Speed, 80 ft/sec.

Figure 12.- Longitudinal section through planes of symmetry showing contours of constant-speed ratio.

[redacted]

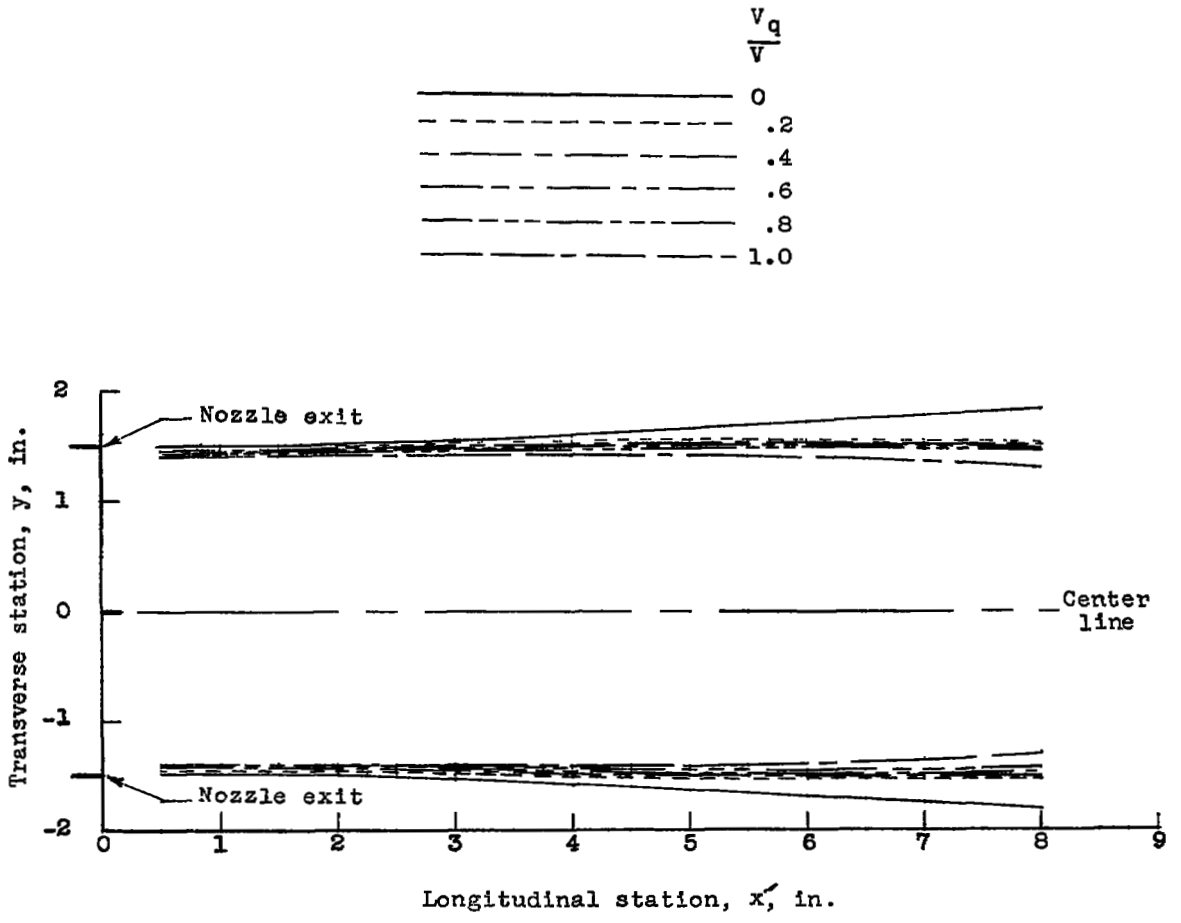

(b) Speed, 130 ft/sec.

Figure 12.- Continued.

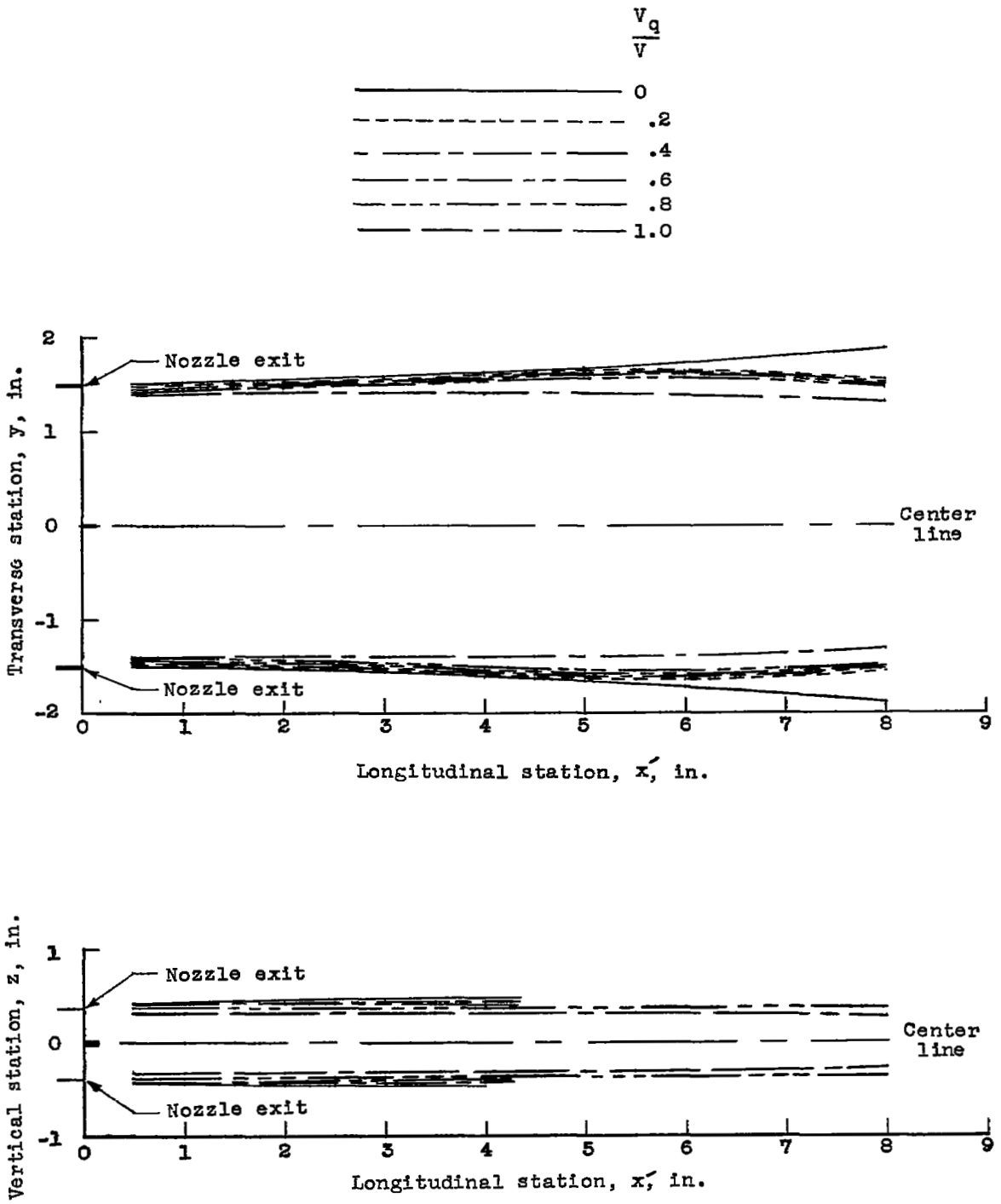

(c) Speed, 200 ft/sec.

Figure 12.- Concluded.

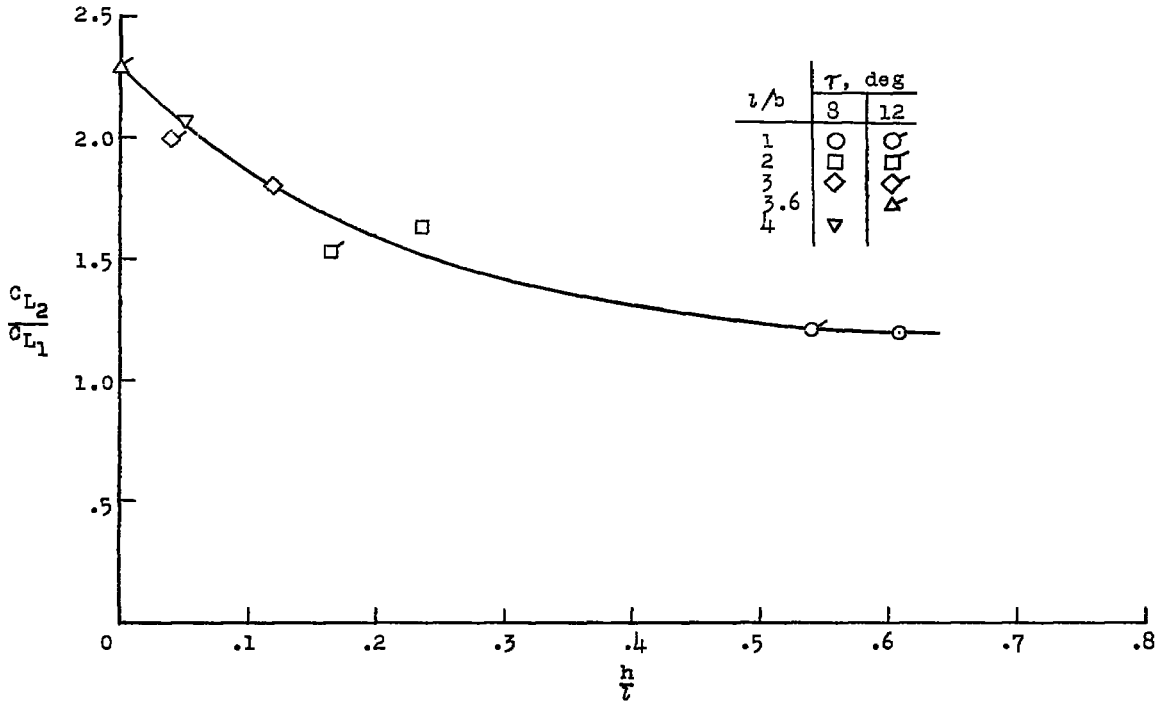

Figure 13.- Ratio of flat-bottom-model hydrodynamic lift coefficients obtained in the tank to those obtained in the jet. V = 80 ft/sec.

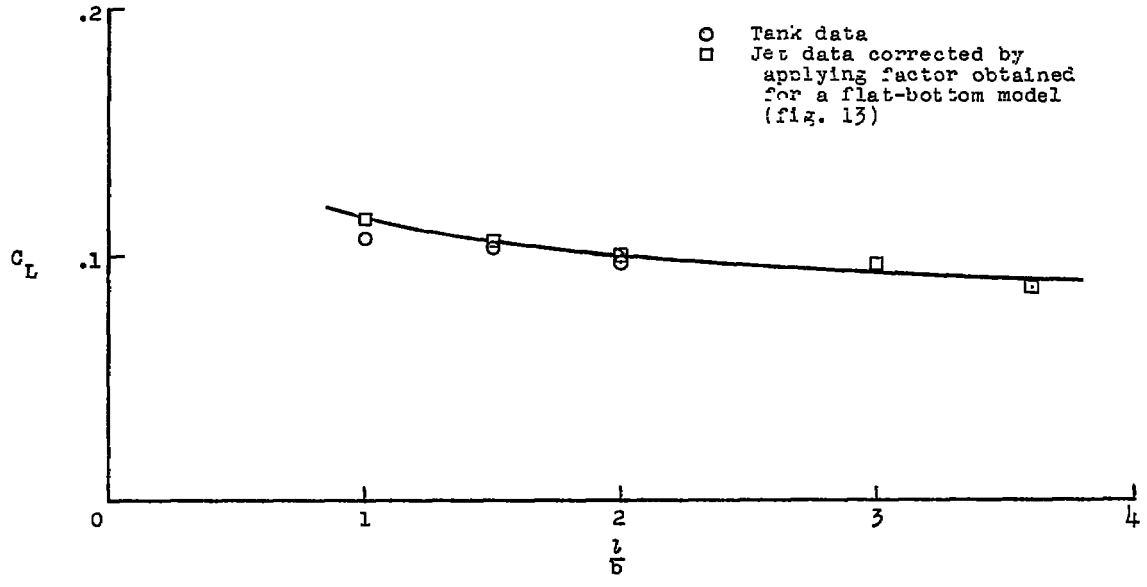

Figure 14.- Comparison of complex-bottom-model hydrodynamic lift data obtained in the tank with the data obtained in the jet. $\tau = 9^\circ$; V = 80 ft/sec.

[redacted]

NACA-Langley - 6-14-54 - 850